Available online at www.sciencedirect.com

ScienceDirect

IFAC Papers Online CONFERENCE PAPER ARCHIVE

IFAC PapersOnLine 54-21 (2021) 1–6

Gaussian Process based Model Predictive Control to address uncertain milling circuit dynamics

Laurentz E. Olivier *,**

* *Analyte Control, Pretoria, South Africa (e-mail: LaurentzO@analyte.co.za).*

** *University of Pretoria, Pretoria, 0002, South Africa.*

Abstract: Model predictive control performance rests heavily on the accuracy of the available plant model. To address (possibly) time-variant model uncertainty, a nominal nonlinear state-space model is combined with an additive residual model that takes the form of a Gaussian process. With sufficient operational data the Gaussian process model is able to effectively describe the residual model error and reduce the overall prediction error for effective model predictive control. The efficacy of the method is illustrated using a milling circuit simulator.

Keywords: Gaussian process, milling, model predictive control, model uncertainty, run-of-mine ore.

1. INTRODUCTION

Model predictive control (MPC) is the most successful form of advanced control used in the process industries (Samad, 2016; Bauer and Craig, 2008). MPC performance is however largely dependent on the accuracy of the plant model that is available (Camacho and Bordons, 2012), but plant models are often uncertain and may change over time.

Poor process modelling is one of the three difficulties that Hodouin (2011) lists for controlling minerals processing plants. In fact, Hodouin (2011) goes on to note that peripheral control tools are as important as the controller itself in minerals processing applications, where peripheral control tools are all the elements in the control loop (apart from the controller itself) that contribute to improving controller performance. Peripheral control tools that mitigate the effects of model-plant mismatch (MPM) is therefore topical.

Detecting MPM has been illustrated by e.g. Badwe et al. (2009) and in the minerals processing industry by e.g. Olivier and Craig (2013). MPM detection however only indicates a problem, but does not directly alleviate the problem. Further analysis can be performed to compensate directly for MPM that may be present.

It is not straightforward to obtain accurate nonlinear dynamic models for process control (Henson, 1998). It may be easier to derive a simplified process model and exploit available measurement data to enhance the system model and hence the controller performance (Hewing et al., 2019). Non-parametric methods, that are widely applied in machine learning, have some potential appeal for application in this area (Pillonetto et al., 2014).

Kocijan et al. (2004) shows and early application of a GP model to MPC. The particular appeal of GP models is that they provide information about prediction uncertainties, that are difficult to obtain directly from some other nonlinear parametric models. Hewing et al. (2019) shows how a nominal system model can be combined with an additive nonlinear component, which is modelled as a Gaussian process (GP), to improve overall control performance. Ostafew et al. (2016) shows how the control response time can be reduced when the error is large and increased as the error decreases. Yang and Maciejowski (2015) shows GP-based MPC to achieve fault-tolerant control.

Run-of-mine (ROM) ore milling is generally the first, and most expensive, unit operation in the metallurgical extraction process (Craig and MacLeod, 1995). Apart from the aforementioned modelling difficulties in minerals processing, mill discharge specifications (chiefly the particle size distribution) needs to remain under tight control to aid downstream extraction (Wei and Craig, 2009). Even though MPC can in general provide such tight control, MPM may be severe enough to inhibit the controller from achieving this goal.

This paper presents a GP-based MPC implementation, applied to a milling circuit simulator, to illustrate how overall control performance may be improved when the GP regression model improves the MPC predictions.

The GP-based MPC formulation, along with the computational considerations for its evaluation, are presented in Section 2. The milling circuit model is described in Section 3, with the simulation setup and results in Section 5, and finally the conclusion in Section 6.

2. GP-BASED MPC

This section describes the composition of the GP-based MPC formulation. The standard MPC formulation is presented first, followed by the GP model for the residual.

10.1016/j.ifacol.2021.12.001

Lastly the two are combined, with some computational consideration, into the final GP-based MPC.

2.1 System model

Consider the general discrete time state-space representation of a dynamic system

$$x_{k+1} = f\left(x_k, u_k, \theta_k, v_k\right) \tag{1}$$
$$y_k = g\left(x_k, u_k, \theta_k, d_k, n_k\right) \tag{2}$$

where $x \in \mathbb{R}^n$ is the state vector and $y \in \mathbb{R}^m$ is the output vector, $f(\cdot)$ and $g(\cdot)$ are possibly nonlinear functions describing the state transitions and the outputs respectively, k the current time step, u_k contains the exogenous inputs, θ_k represents the system parameters, $d_k \in \mathbb{D}$ represents the modelled disturbances, v_k is the state noise, and n_k is the measurement noise.

2.2 Standard MPC formulation

Considering the system presented in equations (1) and (2), the objective of a model predictive controller at each sampling instant is to minimise the scalar performance index

$$\begin{aligned} \min_{u_k \dots u_{k+N_c-1}} \quad & J(u_k, \dots, u_{k+N_c-1}, x_k, r) \\ s.t. \quad & x_{k+1} = f\left(x_k, u_k, \theta_k, v_k\right) \\ & y_k = g\left(x_k, u_k, \theta_k, d_k, n_k\right) \\ & \theta_c(y_k \dots y_{k+N_p}, u_k \dots u_{k+N_c-1}) \leq 0 \end{aligned} \tag{3}$$

where $x : \mathbb{R} \to \mathbb{R}^{n_x}$ is the state trajectory, $u : \mathbb{R} \to \mathbb{R}^{n_u}$ is the control trajectory, x_k is the state at time step k, r is the reference signal (which may in general specify manipulated variable or controlled variable targets), and $\theta_c(\cdot)$ is a possibly nonlinear constraint function.

The performance index (or objective function) to be minimised penalises output values different from the reference values, as well as excessive control moves. The flexibility with which control objectives can be incorporated into the objective function is partly why MPC is such a popular technology. The objective function used in this work is:

$$\begin{aligned} J(\cdot) = & \sum_{i=1}^{N_p} \left[\|y_{r,i} - \hat{y}_i + D\|_{Q_r}^2 + Q_l y_i \right] \\ & + \sum_{i=0}^{N_c-1} \|\Delta u_i\|_R^2 \end{aligned} \tag{4}$$

where N_p and N_c are the prediction and control horizons respectively; $\|\cdot\|_Q^2$ is the Q-weighted 2-norm; Q_r, Q_l, and R are weighting matrices corresponding to the reference tracking, linear optimization objectives (LP weights), and control movements; y_r is the output reference and $\hat{y}$ is the output prediction.

If any plant output variable does not have a specific reference value, but should rather be minimized, the corresponding entry in the Q_r matrix could be made zero while the corresponding entry in the Q_l matrix is given a positive weighting value (or negative if the value should be maximized).

The term, $D = y_k - \hat{y}_k$ (which is constant over the prediction horizon), is included to add integral action (i.e. zero off-set tracking) to the MPC, where y_k is the plant output and $\hat{y}_k$ is the model output at time step k. This conventional feedback procedure assumes the difference between the process and model outputs is because of additive output disturbances, which persist throughout the prediction horizon (Meadows and Rawlings, 1997). Although this method can be sensitive to fluctuations in the output, it is a simple yet effective method for compensating the effects of output disturbances.

2.3 Gaussian process regression

The Gaussian process for modelling the residual dynamics is accomplished first by adapting the process model formulation of (1) to be

$$x_{k+1} = f\left(x_k, u_k, \theta_k\right) + B_d\left(h\left(x_k, u_k\right) + v_k\right) \tag{5}$$

where $h\left(\cdot\right)$ describes the initially unknown dynamics of the system, that are to be learned from data, and are assumed to lie in the subspace spanned by B_d.

Gaussian process regression is then used to infer the function $h\left(\cdot\right)$ from previously collected operating data (including states and inputs). The GP model outputs are obtained from the residual of the measurements and the nominal system model

$$z_k = h\left(x_k, u_k\right) + v_k \tag{6}$$
$$= B_d^+\left(x_{k+1} - f\left(x_k, u_k, \theta_k\right)\right) \tag{7}$$

where B_d^+ is the Moore-Penrose pseudo-inverse. Using a GP prior for $h\left(\cdot\right)$ in each output dimension (as each dimension is modelled separately) gives

$$\mathbf{h}_a \mid \mathbf{z} \sim \mathcal{GP}\left(m_a(z), k_a(z, z')\right) \tag{8}$$

where $a \in [1, \dots, n_d]$ with n_d the number of GP outputs, $m_a(z)$ and $k_a(z, z')$ are any valid functions that evaluate the mean and covariance of $\mathbf{h}_a$. Here the zero mean ($m(z) = 0$) and square exponential kernel (SE)

$$k(z, z') = \sigma_f^2 \exp\left(-\frac{1}{2}\left(z - z'\right)^T M^{-1}\left(z - z'\right)\right) \tag{9}$$

are used, with $\sigma_f^2 \in \mathbb{R}^{1 \times n_z}$ and $M \in \mathbb{R}^{n_z \times n_z}$ the squared output variance and length-scale covariance matrix respectively.

2.4 GP-based MPC formulation

Given the redefinition of the state equations in (5) the MPC formulation can now be adapted as

$$\begin{aligned} \min_{u_k \dots u_{k+N_c-1}} \quad & J(u_k, \dots, u_{k+N_c-1}, x_k, r) \\ s.t. \quad & x_{k+1} = f\left(x_k, u_k, \theta_k\right) + B_d \mu_k^d \\ & y_k = g\left(x_k, u_k, \theta_k, d_k, n_k\right) \\ & \theta_c(y_k \dots y_{k+N_p}, u_k \dots u_{k+N_c-1}) \leq 0 \end{aligned} \tag{10}$$

where the state equation of (5) is used, but because of the GP the predictions are now random variables.

2.5 Computational considerations

The evaluation of (5) is however intractable (Hewing et al., 2019), and the workaround used here is to evaluate it using an Extended Kalman Filter like approach to first linearize (5) with respect to the random variables around the mean as

$$\begin{aligned} f\left(x_k, u_k, \theta_k\right) \approx & \; f\left(\mu^x, \mu^u\right) \\ & + \nabla f\left(\mu^x, \mu^u\right)\left(\begin{bmatrix} x \\ u \end{bmatrix} - \begin{bmatrix} \mu^x \\ \mu^u \end{bmatrix}\right) \end{aligned} \tag{11}$$

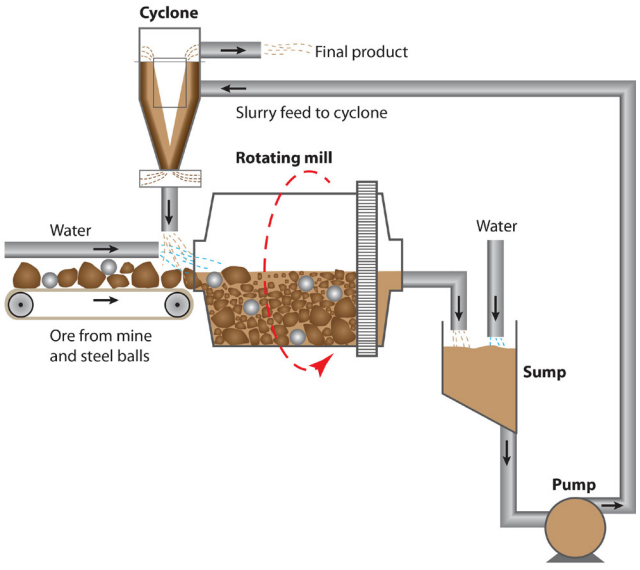

Fig. 1. ROM ore milling circuit layout.

and use simple update equations for the state mean and variance based on affine transformations of the Gaussian distribution

$$\mu^x_{k+1} = f\left(\mu^x, \mu^u\right) + B_d \mu^d_i \tag{12}$$
$$\Sigma^x_{k+1} = \left[\nabla f\left(\mu^x, \mu^u\right) B_d\right] \Sigma_k \left[\nabla f\left(\mu^x, \mu^u\right) B_d\right]^T. \tag{13}$$

This is a computationally cheap approach to evaluate this intractable MPC formulation (Hewing et al., 2019).

The amount of operating data to include in the GP model dictionary is a tuning parameter of the model. Keeping more operational data may improve the prediction accuracy, but means that the model will be more sluggish to react to changing dynamics. The number of data-points to keep will therefore be a function of the rate at which system dynamics are expected to change as well as the computational load of evaluating the model with more data. Here 100 data-points are used.

3. MILLING CIRCUIT MODEL

The milling circuit model used is fully described in Le Roux et al. (2013), although a shortened description is provided next for completeness. The milling circuit is shown in Fig. 1.

The inputs into the milling circuit are the mill water feed (MIW), mill feed ore (MFS), mill steel balls feed (MFB), the sump water feed (SFW), the cyclone feed flow-rate (CFF), and the speed of turning of the mill (α_{speed}) which can be included if the mill motor is fitted with a variable speed drive (as assumed here). The milling circuit outputs are the mill load (LOAD), sump volume (SVOL), particle size estimate (PSE), circuit throughput (THP), and the mill power draw (P_{mill}).

The mill state transitions are given by:

$$\begin{aligned}
\dot{X}_{mw} &= MIW - V_{mwo} \\
\dot{X}_{ms} &= (1-\alpha_r)\frac{MFS}{D_s} - V_{mso} + RC \\
\dot{X}_{mf} &= \alpha_f \frac{MFS}{D_s} - V_{mfo} + FP \\
\dot{X}_{mr} &= \alpha_r \frac{MFS}{D_s} - RC \\
\dot{X}_{mb} &= \frac{MFB}{D_b} - BC,
\end{aligned} \tag{14}$$

with

$$\begin{aligned}
V_{mwo} &= V_V \cdot \varphi \cdot X_{mw} \left(\frac{X_{mw}}{X_{mw}+X_{ms}}\right) \\
V_{mso} &= V_V \cdot \varphi \cdot X_{mw} \left(\frac{X_{ms}}{X_{mw}+X_{ms}}\right) \\
V_{mfo} &= V_V \cdot \varphi \cdot X_{mw} \left(\frac{X_{mf}}{X_{mr}+X_{ms}}\right)
\end{aligned} \tag{15}$$

$$BC = \frac{1}{D_b \phi_b} \cdot P_{mill} \cdot \varphi \cdot \left(\frac{X_{mb}}{X_{mb}+X_{mr}+X_{ms}}\right) \tag{16}$$

$$RC = \frac{1}{D_s \phi_r} \cdot P_{mill} \cdot \varphi \cdot \left(\frac{X_{mr}}{X_{mr}+X_{ms}}\right) \tag{17}$$

$$FP = \frac{P_{mill}}{D_s \phi_f \left[1 + \alpha_{\phi_f}\left(\frac{LOAD}{v_{mill}} - v_{P_{max}}\right)\right]} \tag{18}$$

$$\varphi = \left(\frac{\max\left[0, \left(X_{mw} - \left(\frac{1}{\varepsilon_{ws}} - 1\right) X_{ms}\right)\right]}{X_{mw}}\right)^{0.5} \tag{19}$$

$$P_{mill} = P_{max} \cdot \left\{1 - \delta_{P_v} Z_x^2 - \delta_{P_s} Z_r^2\right\} \cdot \left(\alpha_{speed}\right)^{\alpha_P} \tag{20}$$

$$Z_x = \frac{LOAD}{v_{P_{max}} \cdot v_{mill}} - 1 \tag{21}$$

$$Z_r = \frac{\varphi}{\varphi_{P_{max}}} - 1. \tag{22}$$

The sump state transition equations are:

$$\begin{aligned}
\dot{X}_{sw} &= V_{mwo} + SFW - V_{swo} \\
\dot{X}_{ss} &= V_{mso} - V_{sso} \\
\dot{X}_{sf} &= V_{mfo} - V_{sfo}
\end{aligned} \tag{23}$$

with

$$\begin{aligned}
V_{swo} &= CFF \cdot \left(\frac{X_{sw}}{X_{ss}+X_{sw}}\right) \\
V_{sso} &= CFF \cdot \left(\frac{X_{ss}}{X_{ss}+X_{sw}}\right) \\
V_{sfo} &= CFF \cdot \left(\frac{X_{sf}}{X_{ss}+X_{sw}}\right).
\end{aligned} \tag{24}$$

The cyclone is described as:

$$V_{ccu} = \left(V_{sso} - V_{sfo}\right) \cdot \left(1 - C_1 \cdot e^{-\frac{CFF}{\varepsilon_c}}\right) \cdot \left(1 - \left[\frac{F_i}{C_2}\right]^{C_3}\right) \cdot \left(1 - P_i^{C_4}\right) \tag{25}$$

$$V_{cwu} = V_{swo} \cdot \frac{V_{ccu} - F_u \cdot V_{ccu}}{F_u \cdot V_{swo} + F_u \cdot V_{sfo} - V_{sfo}} \tag{26}$$

$$V_{cfu} = V_{sfo} \cdot \frac{V_{ccu} - F_u \cdot V_{ccu}}{F_u \cdot V_{swo} + F_u \cdot V_{sfo} - V_{sfo}} \tag{27}$$

$$F_u = 0.6 - (0.6 - F_i) \cdot e^{-\frac{V_{ccu}}{\alpha_{su}\varepsilon_c}}, \tag{28}$$

Table 1. Parameters and constants contained in the milling circuit equations.

Parameter	Value	Description
α_f	0.055	Fraction of fines in the ore
α_r	0.465	Fraction of rocks in the ore
ϕ_f	29.57	Power per ton of fines produced $[\frac{\text{kW}\cdot\text{h}}{\text{t}}]$
ϕ_r	6.03	Rock abrasion factor $[\frac{\text{kW}\cdot\text{h}}{\text{t}}]$
ϕ_b	90	Steel abrasion factor $[\frac{\text{kW}\cdot\text{h}}{\text{t}}]$
ε_{ws}	0.6	Maximum water-to-solids volumetric flow at zero slurry flow
V_V	84	Volumetric flow per "flowing volume" driving force $[\text{h}^{-1}]$
P_{max}	1661	Maximum mill motor power [kW]
δ_{P_v}	0.5	Power change parameter for volume of mill filled
δ_{P_s}	0.5	Power change parameter for fraction solids in the mill
$v_{P_{max}}$	0.34	Fraction of mill volume filled for maximum power
$\varphi_{P_{max}}$	0.57	Rheology factor for maximum mill power
α_P	1.0	Fractional power reduction per fractional reduction from maximum mill speed
v_{mill}	59.1	Mill volume $[\text{m}^3]$
α_{ϕ_f}	0.01	Fractional change in kW/fines produced per change in fractional filling of mill
ε_c	128.85	Coarse split parameter
α_{su}	0.87	Parameter related to solids in cyclone underflow
C_1	0.6	Constant
C_2	0.7	Constant
C_3	4	Constant
C_4	4	Constant

$$F_i = \frac{V_{sso}}{V_{swo} + V_{sso}} \tag{29}$$

$$P_i = \frac{V_{sfo}}{V_{sso}}. \tag{30}$$

with $V_{cfo} = V_{sfo} - V_{cfu}$ and $V_{cco} = (V_{sso} - V_{sfo}) - V_{ccu}$.

The milling circuit outputs are then given by:

$$\begin{aligned} LOAD &= X_{mw} + X_{ms} + X_{mr} + X_{mb} \\ SVOL &= X_{sw} + X_{ss} \\ PSE &= \frac{V_{cfo}}{V_{cco} + V_{cfo}} \\ THP &= V_{cco} + V_{cfo} \end{aligned} \tag{31}$$

as well as P_{mill} given in (20). The parameter values contained in the process equations are listed in Table 1 (units are shown next to parameters that are not dimensionless).

In the simulations that follow, the system equations are progressed using the Runge-Kutta 4^{th} order method and a sampling rate of 10 seconds.

4. CONTROLLER DESIGN

The output vector is given by

$$y = \begin{bmatrix} LOAD \\ SVOL \\ PSE \\ THP \\ P_{mill} \end{bmatrix} \tag{32}$$

and the input vector is given by

$$u = \begin{bmatrix} MIW \\ MFS \\ MFB \\ SFW \\ CFF \\ \alpha_{speed} \end{bmatrix}. \tag{33}$$

The design parameters required for the MPC are the Q_r, Q_l, and R tuning weights. Q_r is

$$Q_r = \begin{bmatrix} 4 & 0 & 0 & 0 & 0 \\ 0 & 0 & 0 & 0 & 0 \\ 0 & 0 & 5e3 & 0 & 0 \\ 0 & 0 & 0 & 0 & 0 \\ 0 & 0 & 0 & 0 & 0 \end{bmatrix} \tag{34}$$

which shows that PSE control is the most important reference tracking objective. The LOAD has a weak reference tracking weight as there is some indication that an optimal LOAD value for maximum breakage exists.

The Q_l weighting matrix is given by

$$Q_l = \begin{bmatrix} 0 & 0 & 0 & 0 & 0 \\ 0 & 0 & 0 & 0 & 0 \\ 0 & 0 & 0 & 0 & 0 \\ 0 & 0 & 0 & -1 & 0 \\ 0 & 0 & 0 & 0 & 1 \end{bmatrix} \tag{35}$$

which indicates that the throughput should be maximized while the mill power should be minimized.

These objectives are in contrast with each other as increasing throughput generally requires increased breakage which generally requires increased mill power draw. However, the objectives are traded off against each other by the relative values of the tuning weights.

The manipulated variable move weights (R) are given by

$$R = \begin{bmatrix} 0.4 & 0 & 0 & 0 & 0 & 0 \\ 0 & 0.08 & 0 & 0 & 0 & 0 \\ 0 & 0 & 12.5 & 0 & 0 & 0 \\ 0 & 0 & 0 & 0.002 & 0 & 0 \\ 0 & 0 & 0 & 0 & 0 & 0 \\ 0 & 0 & 0 & 0 & 0 & 200 \end{bmatrix} \tag{36}$$

where (again) the relative values are important. E.g. SFW is allowed to move much more than α_{speed}.

The controller manipulated variable low and high limits are given by

$$\underline{U} = [0, 0, 0, 0, 200, 0.4]^T \tag{37}$$

and

$$\overline{U} = [50, 200, 10, 300, 450, 1]^T. \tag{38}$$

5. SIMULATION RESULTS

The simulation setup is described first, before the simulation results are presented and discussed.

5.1 Simulation setup

The nominal parameter values used in the simulation are as shown in Table 1. After 1 hour the PSE setpoint is increased by 10%. Such a PSE setpoint change is not very common apart from instances where the downstream particle size distribution requirement for recovery has changed. Here, the setpoint change is however used to

illustrate the reference tracking capability of the controller, as the PSE reference is the most important controlled variable.

Some model-plant mismatch is introduced to illustrate the working of the GP model. The parameter α_f in (14) is adapted to be

$$\alpha_f^* = \tilde{\alpha}_f \cdot \alpha_f \tag{39}$$

where α_f is the nominal value as shown in Table 1 and $\tilde{\alpha}_f$ is defined as

$$\tilde{\alpha}_f = \text{mid}\left(-0.8, \lambda_1 \left(MFS - \lambda_2\right), 0\right) \tag{40}$$

where $\lambda_1 = 3$ is a scaling constant and $\lambda_2 = 60$ is close to the steady-state solids feed; $\text{mid}\left(\cdot,\cdot,\cdot\right)$ is a middle of three function that is used to clamp a value between a lower and upper limit. This adaptation implies that as the feed increases the fraction of fines in the feed ore increases. This type of scenario can happen with feed from a stockpile with multiple feeders, where the particle size distribution of the separate sections of the stockpile where feed is taken from are different.

As the feed increases the fraction of fines in the feed also increases. This implies that the holdup of fines in the mill will increase (state number 3 - X_{mf}).

A decent amount of measurement noise is also added to reinforce the fact that the method works with noisy operating data. The measurement noise standard deviations are

$$\sigma_y = \text{diag}\left(\frac{1}{1000} \; \frac{1}{5} \; \frac{1}{180} \; \frac{1}{5} \; \frac{1}{0.1}\right), \tag{41}$$

where $\text{diag}(\cdot)$ is the diagonal matrix. The standard deviations were chosen such that the noise would visually appear significant.

At first, the nominal model as described in Section 3 is used in the MPC without the GP model active. The simulation result illustrating the control performance with the nominal model used for predictions is shown in Fig. 2.

Next, the GP model is included. As the fraction of fines in the feed change exists in the plant, but not in the process model used by the MPC, the GP should model this uncertainty and help improve predictions. The simulation result for this scenario is shown in Fig. 4.

5.2 Simulation results discussion

The key values (namely PSE, LOAD, and throughput) are shown without the GP model active in Fig. 2. For the PSE and LOAD the setpoint is indicated with the red dashed line. For the throughput there is no setpoint, but the red dashed line is included as a baseline value.

Some time is needed to attain steady-state from the initial conditions. The PSE setpoint tracking is generally quite good. The LOAD setpoint tracking is not as good, but still fair (given the small weight given to this variable). The throughput is initially relatively high although trending down as X_{mf} is under predicted, but as the PSE setpoint increases the throughput decreases and continues to decrease.

The prediction error (residual) for X_{mf} without the GP model is shown in Fig. 3. As expected, the prediction is generally negative as the solids feed is often below λ_2.

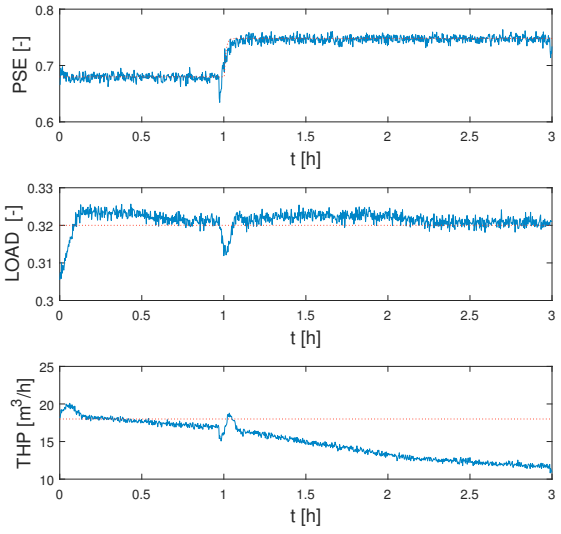

Fig. 2. Key variable results without the GP model active.

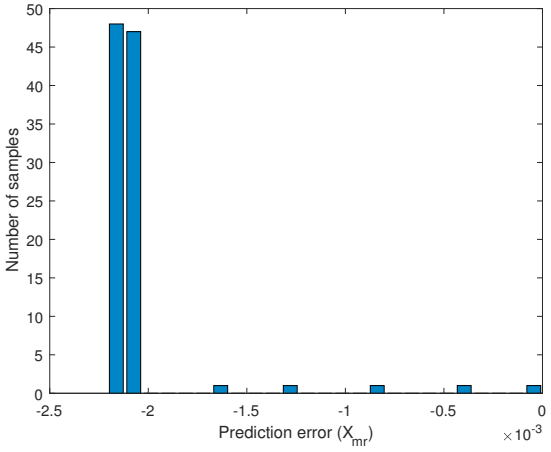

Fig. 3. Prediction error without the GP model active.

When the GP model is active the PSE and LOAD settle out relatively well at setpoint after the initial time required to attain steady-state (see Fig. 4). The PSE setpoint increase does mean that the throughput decreases, but the throughput is maintained at a higher value for longer because of the improved predictions.

The prediction error (residual) for X_{mf} with the GP model is shown in Fig. 5. Now the prediction error is quite closely centred at about 0, implying the GP model is able to improve the prediction accuracy.

The mean absolute error (MAE) from setpoint for the PSE and LOAD along with the mean throughput are shown in Table 2 for the scenarios where the GP is not used and where the GP is used. The % change from not using the GP to using the GP is also shown.

There is an improvement in setpoint tracking for PSE and LOAD when using the GP model, although not that significant. The mean throughput increase of more than 11% is however much more significant.

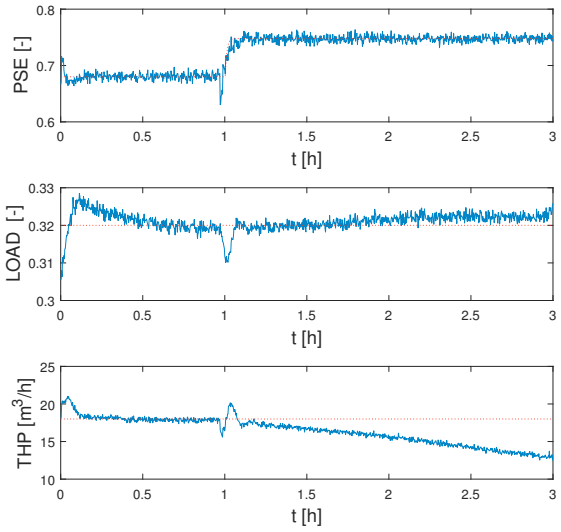

Fig. 4. Key variable results with the GP model active.

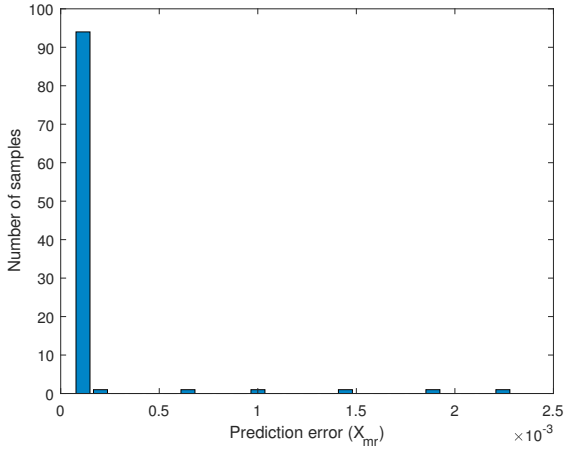

Fig. 5. Prediction error with the GP model active.

Table 2. Evaluation parameters.

Parameter	No GP	With GP	Δ (%)
MAE (PSE)	4.86×10^{-3}	5.09×10^{-3}	4.73%
MAE (LOAD)	1.92×10^{-3}	1.98×10^{-3}	3.13%
Mean THP	14.68	16.40	11.72%

6. CONCLUSION

A GP-based MPC was presented in this work with application to a milling circuit simulator. State value based model-plant mismatch was introduced in the form of the fraction of fines in the feed ore being a function of the amount of fresh feed taken into the mill.

The GP was able to model the residual error resulting from this mismatch, improving controller predictions, and overall control performance. Control performance was improved by mean throughput increasing by more than 11% while still maintaining the PSE and LOAD setpoint tracking.

REFERENCES

Badwe, A.S., Gudi, R.D., Patwardhan, R.S., and Shah, S.L. (2009). Detection of model-plant mismatch in MPC applications. *Journal of Process Control*, 19(8), 1305–1313.

Bauer, M. and Craig, I.K. (2008). Economic assessment of advanced process control – a survey and framework. *Journal of Process Control*, 18(1), 2–18.

Camacho, E.F. and Bordons, C. (2012). *Model predictive control in the process industry*. Springer Science & Business Media.

Craig, I.K. and MacLeod, I.M. (1995). Specificaton framework for robust control of a run-of-mine ore milling circuit. *Control Engineering Practice*, 3, 621 – 630.

Henson, M.A. (1998). Nonlinear model predictive control: current status and future directions. *Computers and Chemical Engineering*, 23(2), 187–202.

Hewing, L., Juraj, K., and Zeilinger, M.N. (2019). Cautious model predictive control using Gaussian process regression. *IEEE Transactions on Control Systems Technology*, 28(6), 2736–2743.

Hodouin, D. (2011). Methods for automatic control, observation, and optimization in mineral processing plants. *Journal of Process Control*, 21, 211 – 225.

Kocijan, J., Murray-Smith, R., Rasmussen, C.E., and Girard, A. (2004). Gaussian process model based predictive control. In *Proceedings of the 2004 American control conference*, volume 3, 2214–2219.

Le Roux, J.D., Craig, I.K., Hulbert, D.G., and Hinde, A.L. (2013). Analysis and validation of a run-of-mine ore grinding mill circuit model for process control. *Minerals Engineering*, 43, 121–134.

Meadows, E.S. and Rawlings, J.B. (1997). *Nonlinear process control*, chapter Model predictive control, 233–310. Prentice Hall, Inc., Upper Saddle River, NJ, USA.

Olivier, L.E. and Craig, I.K. (2013). Model-plant mismatch detection and model update for a run-of-mine ore milling circuit under model predictive control. *Journal of Process Control*, 23(2), 100–107.

Ostafew, C.J., Schoellig, A.P., Barfoot, T.D., and Collier, J. (2016). Learning-based nonlinear model predictive control to improve vision-based mobile robot path tracking. *Journal of Field Robotics*, 33(1), 133–152.

Pillonetto, G., Dinuzzo, F., Chen, T., De Nicolao, G., and Ljung, L. (2014). Kernel methods in system identification, machine learning and function estimation: a survey. *Automatica*, 50(3), 657–682.

Samad, T. (2016). A survey on industry impact and challenges thereof. Available from: http://blog.ifac-control.org/2016/10/03/a-survey-on-industry-impact-and-challenges-thereof/, accessed January 2017.

Wei, D. and Craig, I.K. (2009). Grinding mill circuits – A survey of control and economic concerns. *International Journal of Mineral Processing*, 90(1–4), 56–66.

Yang, X. and Maciejowski, J. (2015). Fault tolerant control using Gaussian processes and model predictive control. *International Journal of Applied Mathematics and Computer Science*, 25, 133–148. doi:10.1515/amcs-2015-0010s.